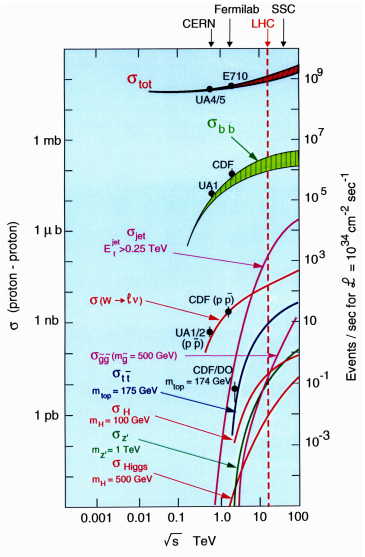

Figure 1: Rates of various processes at hadron colliders vers c.m. energy.

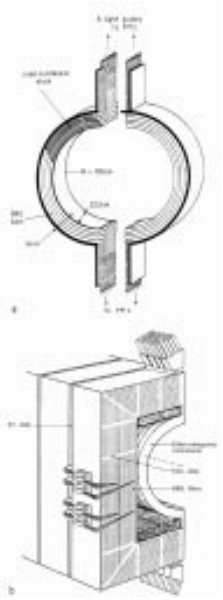

Figure 2: UA1 em gondola calorimeter (top), and hadronic (bottom).

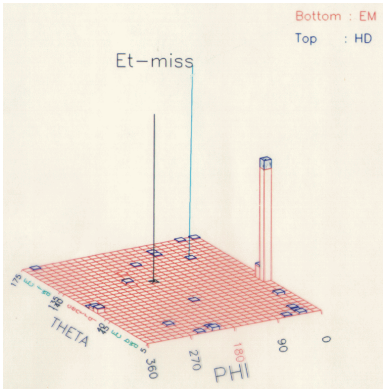

Figure 3: UA2 calorimeter lego plot of W to e ν decay.

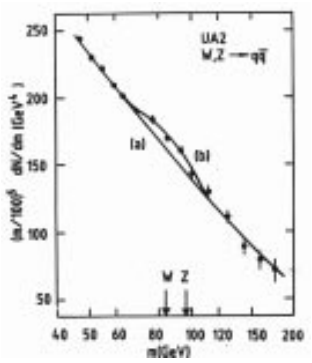

Figure 4: UA2 dijet mass distribution. The W and Z are not resolved.

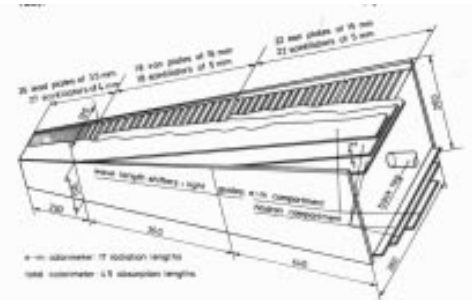

Figure 5: The UA2 calorimeter.

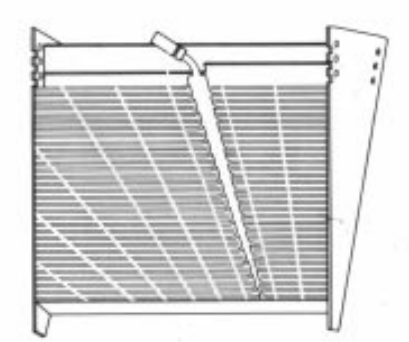

Figure 7: CDF calorimeter principle.

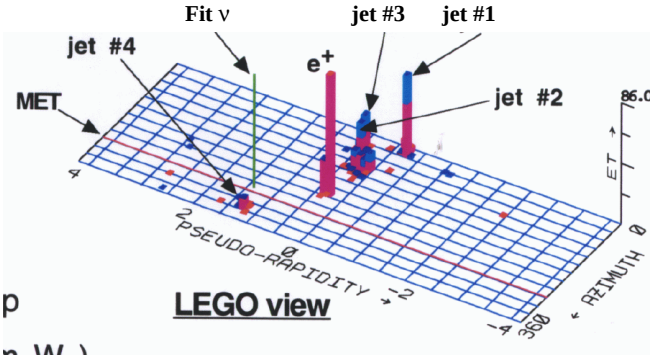

Figure 6: CDF lego plot of a top event $t\bar{t} \rightarrow$ W (e ν) b(jet 1) W (jets 2.3) b(jet 4).

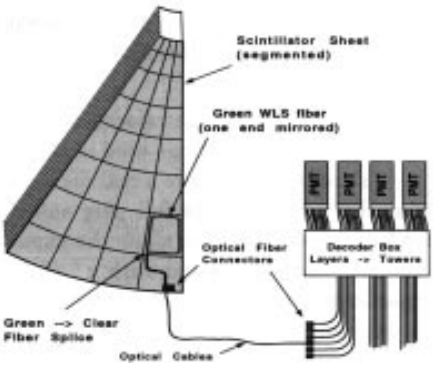

Figure 8: CDF calorimeter upgrade. Principle.

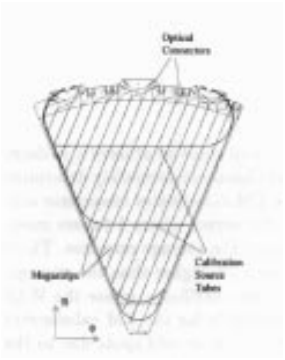

Figure 9: The shower max (SMD) of the CDF upgrade.

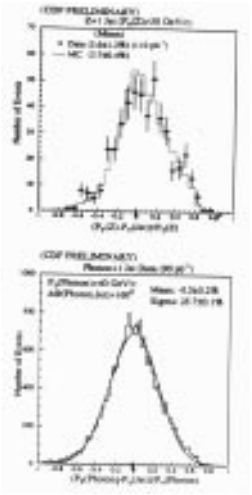

Figure 10: CDF calibration using Z+jets and γ+jet events.

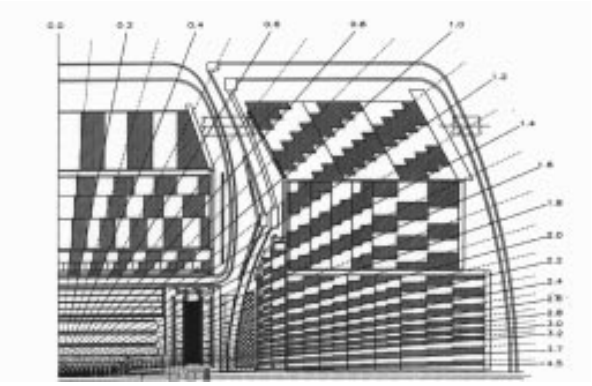

Figure 11: Side view of the D0 calorimeter.

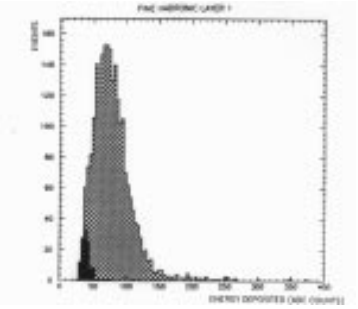

Figure 12 : D0 Noise (black) and μ response.

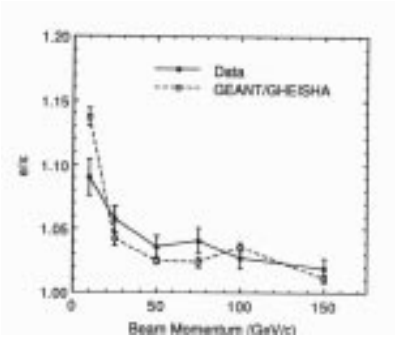

Figure 13: e/π ratio in D0 (data and MC).

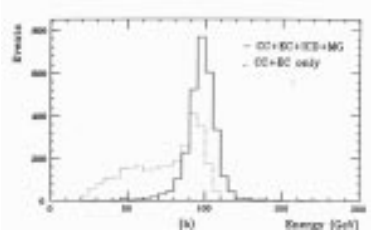

Figure 14: D0 response in the crack with & without MG&ICD info.

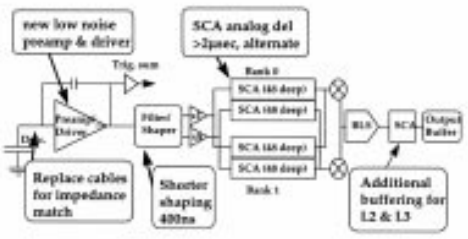

Figure 15: D0 upgrade. Readout scheme.

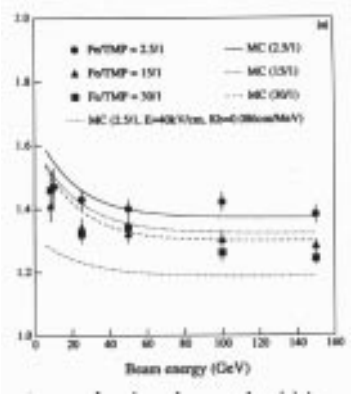

Figure 16: e/π ratio in WALIC.

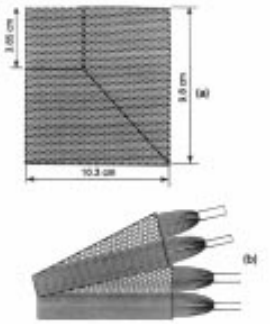

Figure 18: SPACAL projective modules.

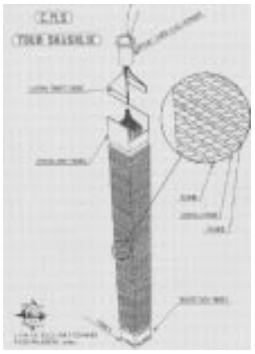

Figure 20: The SHASHLIK calorimeter.

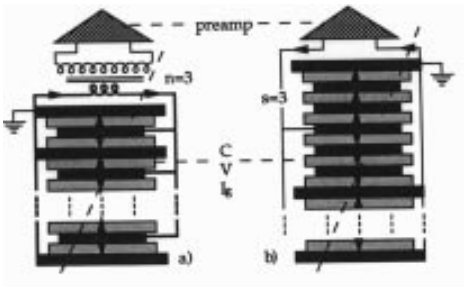

Figure 17: WALIC. The EST transformer readout (a).

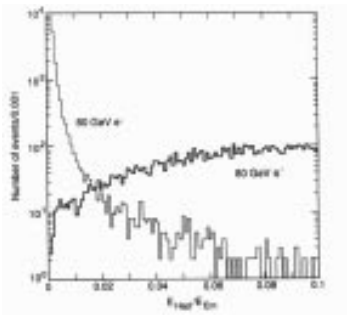

Figure 19: e/π separation in SPACAL.

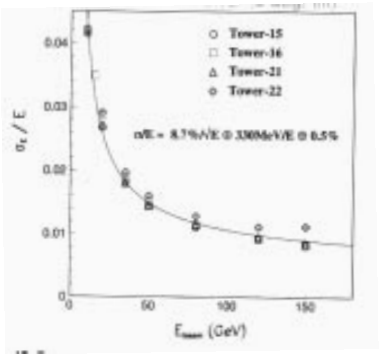

Figure 21: SHASHLIK em energy resolution.

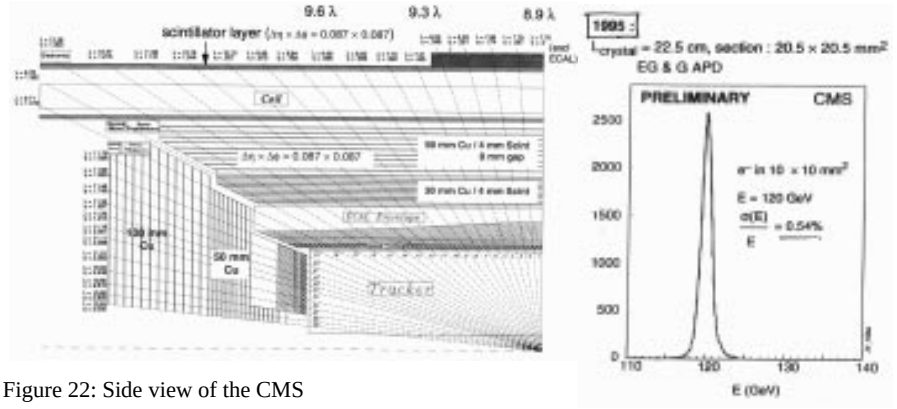

Figure 22: Side view of the CMS calorimetry.

Figure 23: CMS em response using APDs.

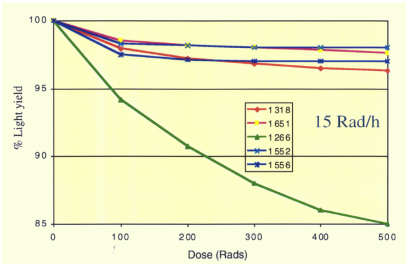

Figure 24: CMS crystals response to irradiation for various stochimetry conditions.

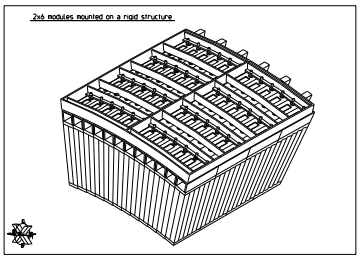

Figure 25: CMS crystals assembly mechanical structure.

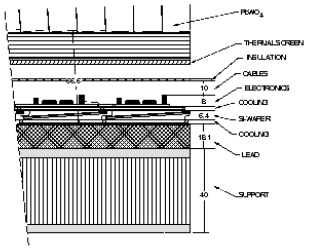

Figure 26: The CMS preshower.

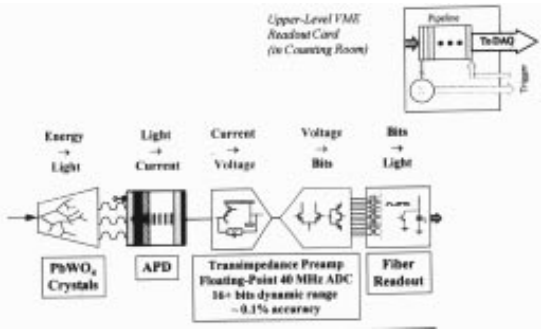

Figure 27: CMS em calorimeter readout.

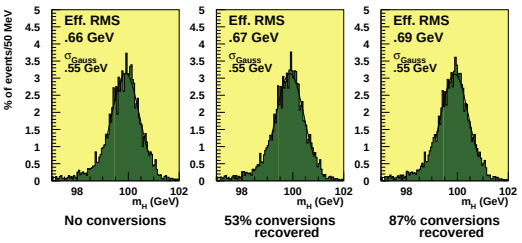

Figure 28: CMS reconstruction of $H \rightarrow \gamma\gamma$, with and without converted photons recovery.

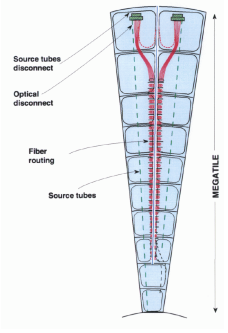

Figure 29: Principle of the CMS hadronic HCAL.

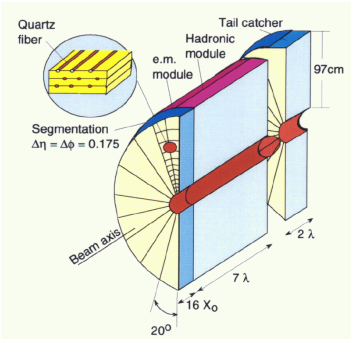

Figure 30: Principle of the CMS very forward calorimeter VFCAL.

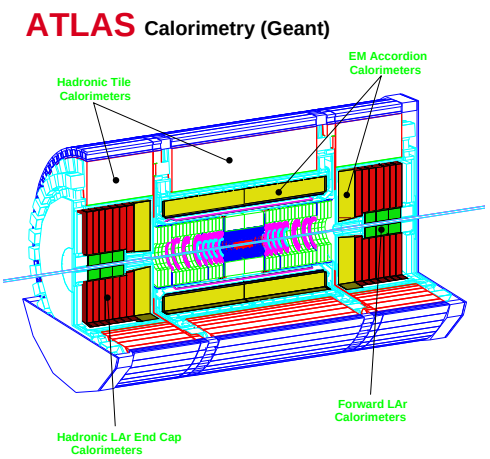

Figure 31: The ATLAS calorimetry (GEANT).

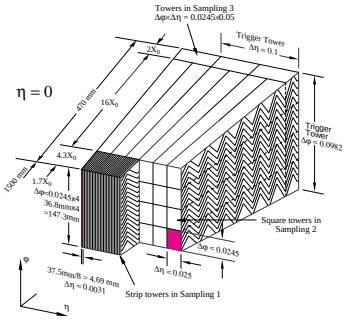

Figure 32: The ATLAS accordion calorimeter structure.

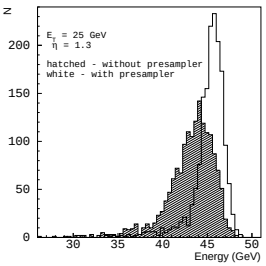

Figure 33: ATLAS em response with the presampler recovery ($|\eta|$=1.3).

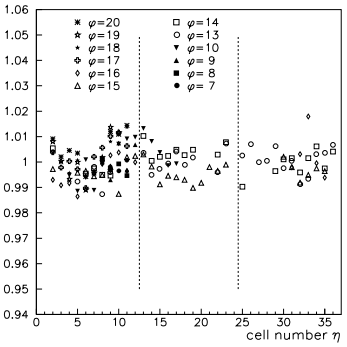

Figure 34: Response uniformity of the ATLAS em calorimeter.

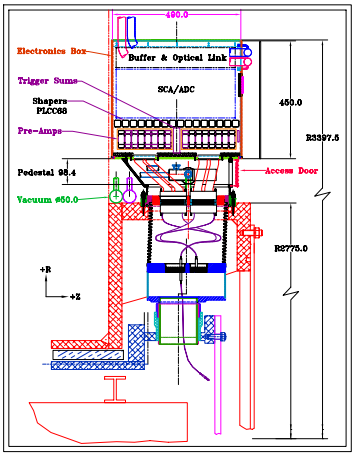

Figure 35: ATLAS em feedthroughs and readout elements.

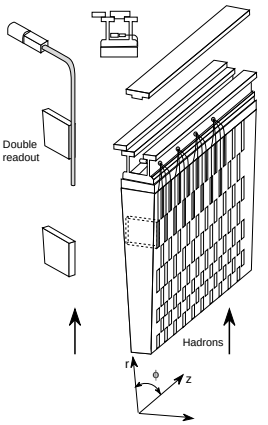

Figure 36:
ATLAS tile calorimeter principle.

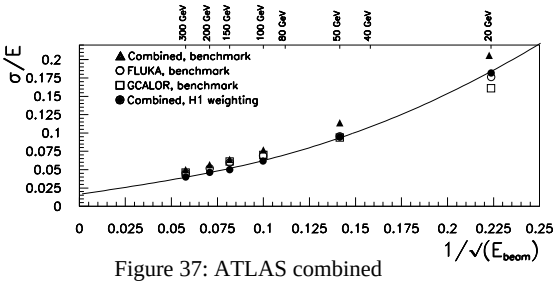

Figure 37: ATLAS combined (em+tile) response to pions. DAta and MC.

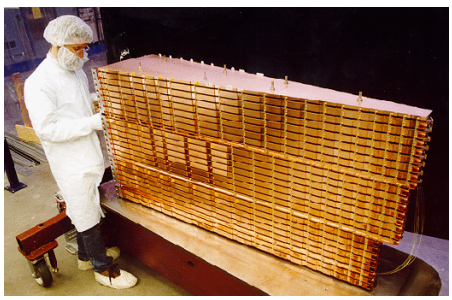

Figure 38: ATLAS HEC prototype.

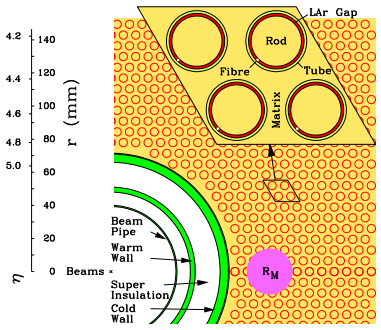

Figure 39: ATLAS FCAL principle.